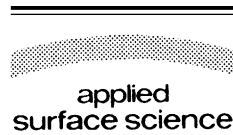




ELSEVIER

Applied Surface Science 194 (2002) 106–111



www.elsevier.com/locate/apsusc

Study of precipitate in Si-rich SiO₂ films

R.S. Brusa^{a,*}, W. Deng^a, G.P. Karwasz^a, A. Zecca^a, G. Mariotto^a,
P. Folegati^b, R. Ferragut^b, A. Dupasquier^b

^aDipartimento di Fisica, Istituto Nazionale per la Fisica della Materia, Università di Trento, 38050 Povo, TN, Italy

^bDipartimento di Fisica, Istituto Nazionale di Fisica della Materia e, Politecnico di Milano, Piazza L da Vinci, 32 20133 Milan, Italy

Abstract

Silicon precipitates have been obtained in layers of Si-rich SiO₂ by ion implantation and thermal treatments. Positron annihilation spectroscopy (PAS) has been used to investigate on open volume defects existing in the oxide; other structural information has been obtained by Raman and Fourier transform infrared (FTIR) spectroscopy. Changes in positronium (Ps) formation and trapping in the implanted layer were observed. The Ps signal decreases after Ar⁺ ion bombardment, which induces a substantial breaking of both Si–H and Si–O bonds. Comparison with Raman measurements suggests that this effect is indirectly related to the formation of Si nano-precipitates. A strong increase of the Ps signal in the implanted samples is observed after thermal treatments at 500 and 800 °C, followed by a new decrease after a thermal treatment at 1100 °C. © 2002 Elsevier Science B.V. All rights reserved.

Keywords: Si-rich silicon oxide; Positron annihilation; Vibrational spectroscopy; Slow positron beam

1. Introduction

The increasing importance of optoelectronics for the communication technologies requires integration of optical devices within microelectronic circuits. Silicon-based optoelectronic components are desirable, as Si is the main material of microelectronic industry; unfortunately, bulk Si is a poor light emitter. Big efforts have been devoted to try to overcome this disadvantage. It was found that Si nano-structures exhibit intense visible light emission. Nano-structures can be produced with several preparation methods (see [1] and references therein), including Si implantation in amorphous SiO₂ matrix [2], and high temperature annealing (1000–1300 °C) of SiO_x films [3,4]. Si

nano-particles embedded in a SiO₂ matrix show photoluminescence in the wavelength range 650–950 nm. The physical mechanism of this effect is not yet fully understood. Some optical phenomena, like the blueshift of the emitted light, are well explained by the band gap widening due to the quantum confinement of the carriers but most experimental data regarding light emission also imply an effect of interfacial electron states (O vacancy, Si=O covalent bond, non-bridging O centres) [2,4,5].

The present work is a preliminary study of SiO_x films modified by Ar bombardment. The energy transfer due to ion bombardment is expected to promote Si precipitation; post-bombardment sample annealing is known to favour the agglomeration of Si. Open volume defects play an important role in transport and clustering processes. Moreover, point defects can be present inside the precipitates and/or at the interface between Si and the embedding matrix, thus

* Corresponding author. Tel.: +39-461-881-552;
fax: +39-461-881-696.
E-mail address: brusa@science.unitn.it (R.S. Brusa).

playing a crucial role in the optical response of the Si nano-structures. Positron spectroscopy has been used to detect the presence of open volume defects in the as-deposited and treated SiO_x samples. Vibrational spectroscopy was employed to detect the formation of Si nano-structures (Raman scattering) and to obtain information about Si–O bonds (Fourier transform infrared (FTIR) spectroscopy).

2. Experimental

The Si-rich silicon oxide films were deposited by plasma-enhanced chemical vapour deposition (PECVD) using p-type Czochralski Si (1 0 0) wafers as substrates (resistivity ≈ 1.7 – $2.5 \Omega \text{ cm}$). The PECVD system was a cold-wall reactor operating at 13.56 MHz radio frequency. Three series of sub-stoichiometric silicon-rich oxide (SiO_x , $x < 2$) films were deposited. Details about sample preparation and characterisation can be found in [6]. In Table 1, we report only the most important characteristics of the samples.

C samples were bombarded with Ar^+ ions with energy of 380 keV and a dose 5×10^{16} ions cm^{-2} , with the Si substrate at room temperature. At 380 keV, the Ar-projected range R_p is about 550 nm, thus the majority of the Ar atoms stops beyond the SiO_x/Si interface. After bombardment, different samples were annealed in vacuum at 500, 800 and 1100 °C for 2 h.

Positron annihilation spectroscopy (PAS) was carried out with a variable energy slow positron beam. A description of the experimental apparatus is reported elsewhere [7,8]. The annihilation line was recorded with a high-purity germanium detector (resolution 1.1 keV for the 356 keV line of Ba^{133} with 2 μs shaping time in the spectroscopy amplifier). The annihilation line was characterised by the S and W parameters, which give information on positron annihilation with electrons of low and high

momentum, respectively. The S parameter is the ratio of the counts in the central area of the peak ($|511 - E\gamma| \leq 0.85 \text{ keV}$) and the total area of the peak ($|511 - E\gamma| \leq 4.25 \text{ keV}$). The energy window for the W parameter (the relative fraction of the counts in the wings region of the annihilation line) was $1.6 \leq |511 - E\gamma| \leq 4.0 \text{ keV}$. The S and W parameter were measured as a function of the positron implantation energy in the 0.06–25 keV range.

Raman spectra were excited at room temperature in nearly backscattering geometry by the 488.0 nm line of an Ar^+ ion laser operated at 300 mW. The scattered radiation was filtered by a double-monochromator (Jobin–Yvon, model Ramanor HG2-S, focal length: 1 m), equipped with holographic gratings (2000 groves mm^{-1}). The signal was detected by a standard photon-counting system. FTIR spectra were recorded in transmission at room temperature using an un-implanted Si wafer as a reference.

3. Results and discussion

The results of PAS measurements are in Figs. 1–3. Fig. 1 shows the S parameter, normalised to the Si bulk S -value, of the as-deposited samples versus the

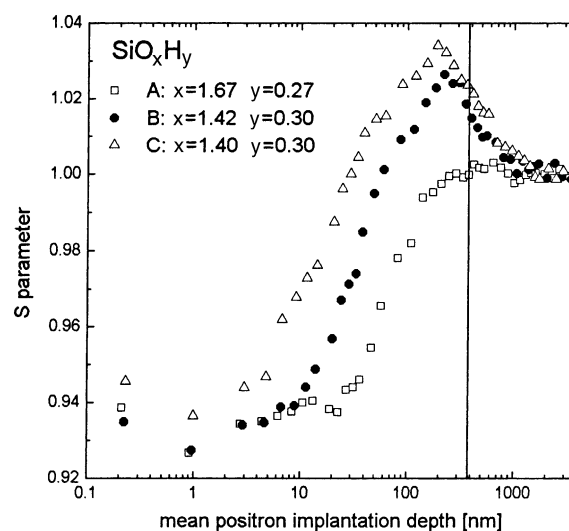


Fig. 1. S parameters of the as-deposited Si-rich SiO_x samples as a function of the mean positron implantation depth. Samples A–C have different Si contents. Vertical line sketches the interface of the SiO_x film with Si.

Table 1
Composition, density and thickness of the samples

Sample series	Composition	Density (g cm^{-3})	Thickness (nm)
A	$\text{SiO}_{1.67}\text{H}_{0.27}$	2.12	356
B	$\text{SiO}_{1.42}\text{H}_{0.30}$	2.00	388
C	$\text{SiO}_{1.40}\text{H}_{0.30}$	1.95	394

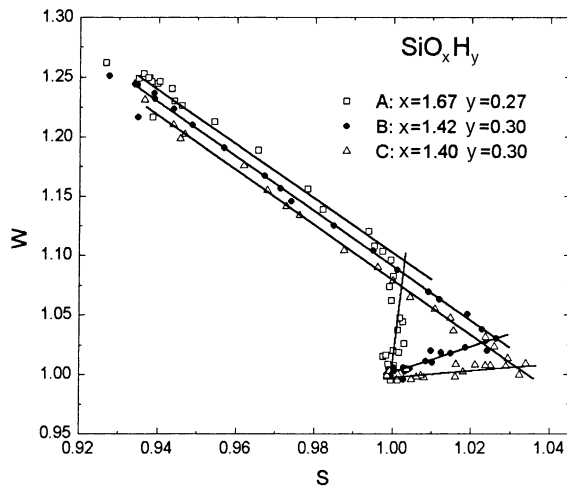


Fig. 2. W vs. S plot for the as-deposited samples.

mean positron implantation depth z . This is calculated according to the equation $z = AE^n / \rho$; where $n = 1.6$, ρ is the density of the films, $A = 4.0 \mu\text{g cm}^{-2} \text{keV}^{-n}$, and E the positron implantation energy. The S -value of the three films begins from a similar surface value ($S \approx 0.94$) and reaches its maximum ($S > 1.0$) just before the interface with Si. A value $S > 1$ would not

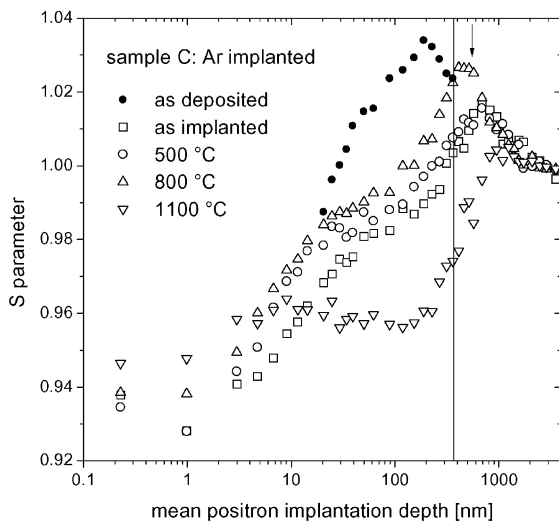


Fig. 3. S parameters of SiO_x samples (C series) Ar^+ -implanted at 380 keV, $5 \times 10^{16} \text{ ions cm}^{-2}$, and thermally treated at 500, 800 and 1100 °C, as a function of the mean positron implantation depth. Vertical line at the interface of the SiO_x film with Si. The arrow indicates the projected range R_p of Ar^+ . For clarity, only a few S values of the as-deposited sample (see Fig. 1) are reported.

be expected for stoichiometric SiO_2 ($S \approx 0.97$ for thermally grown SiO_2 [9]). High S values in Si oxide suggest the presence of positronium (Ps) trapped at open volume defects [10]. Fig. 2 shows the W - S plot [11]. As the positron implantation profile moves from surface to bulk Si passing through the SiO_x layer, the W - S points move from the surface state to the Si bulk state on a trajectory depending on the SiO_x layer conditions. The characteristic W - S point for each film (corresponding to 100% annihilation in the film) can be obtained as the intersection of the tangents of W - S curves at high and low positron implantation energy. The intersection points move toward higher S (~ 1.003 , ~ 1.026 and ~ 1.032) and lower W (~ 1.095 , ~ 1.027 and ~ 1.005) as the density and the relative oxygen content of the film decreases. If one observes that: (a) the increase of S is the symptom of increased Ps formation [10]; (b) the decrease of W indicates reduction of pick-off annihilation with valence electrons of O [12], these trends seem consistent with: (a) increase of the number and the size of the cavities, related to an increased number of Si dangling bonds; (b) decrease of the O concentration on the walls of the cavities.

Ion bombardment produces a drastic decrease of the S values in the film, (compare the as-deposited sample C of Fig. 1 with the as-implanted sample of Fig. 3), in spite a peak immediately beyond the SiO_x/Si interface, which is due to vacancy-like defects produced in the Si substrate by Ar^+ ions. After thermal treatments at 500 and 800 °C, the S parameter increases slightly in the layer (Fig. 3). After annealing at 1100 °C, the S parameter for the film falls to slightly below the indicative S -value of SiO_2 (≈ 0.97 [9]). Also, the radiation damage effects in the Si substrate are strongly reduced. The interpretation of these results can be guided by the results of vibrational spectroscopy.

The results of FTIR and Raman spectroscopy on samples of the C series are shown in Figs. 4 and 5, respectively. The IR absorbance spectrum of as-deposited samples (Fig. 4a) consists of two partly overlapped bands, peaked at ~ 870 and $\sim 1050 \text{ cm}^{-1}$, respectively, and of a broad feature between 2000 and 2300 cm^{-1} . According to [6], the last feature is due to stretching modes of SiH units, the band peaked at $\sim 870 \text{ cm}^{-1}$ is related to bending modes of $\text{O}_3\text{-SiH}$ groups and the one at $\sim 1050 \text{ cm}^{-1}$ is due to SiO-bond stretching vibrations. The intensity of both SiH-bond stretching and $\text{O}_3\text{-SiH}$ bending modes substantially

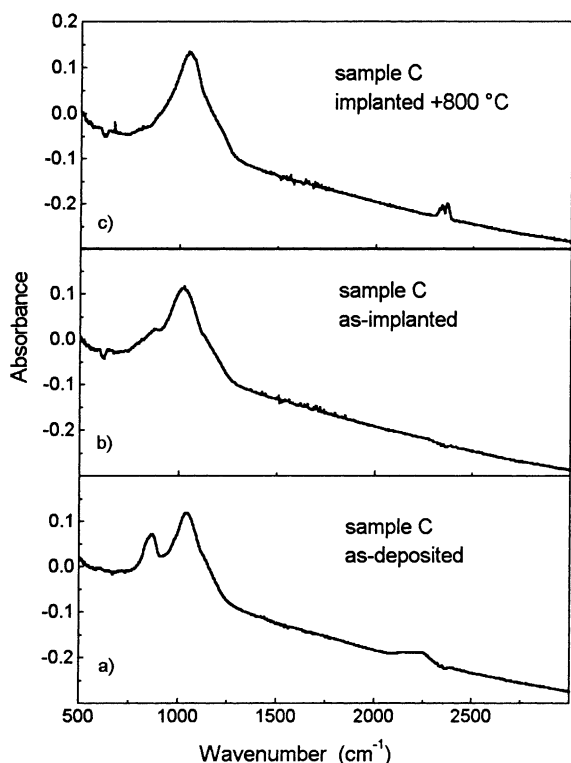


Fig. 4. Infrared spectra for C series samples: (a) as-deposited; (b) as-implanted; (c) as-implanted and thermal treated at 800 °C.

decreases after Ar^+ ion bombardment (Fig. 4b) and almost disappears after annealing at 800 °C (Fig. 4c). Noting that the content of H in the film, as measured by RBS and ERDA, is reduced to one-half after Ar^+ bombardment, the observed behaviour can be ascribed to a substantial breaking of Si–H bonds during ion bombardment, and to the complete destruction of these bonds after thermal annealing at 800 °C. Correspondingly, the main band at $\sim 1050 \text{ cm}^{-1}$ broadens and downshifts to about 1020 cm^{-1} in the as-implanted samples, while in the samples annealed at 800 °C, it appears upshifted to $\sim 1040 \text{ cm}^{-1}$ and slightly narrowed. The broadening of the band due to SiO-bond stretching vibration in as-implanted samples is related to structural disorder induced by the ion bombardment, which also modifies the composition of the film (through the loss of O bonded to Si). Actually, the average composition of the film after implantation by Ar^+ ions results even less stoichiometric than before the implantation, as suggested by the concomitant

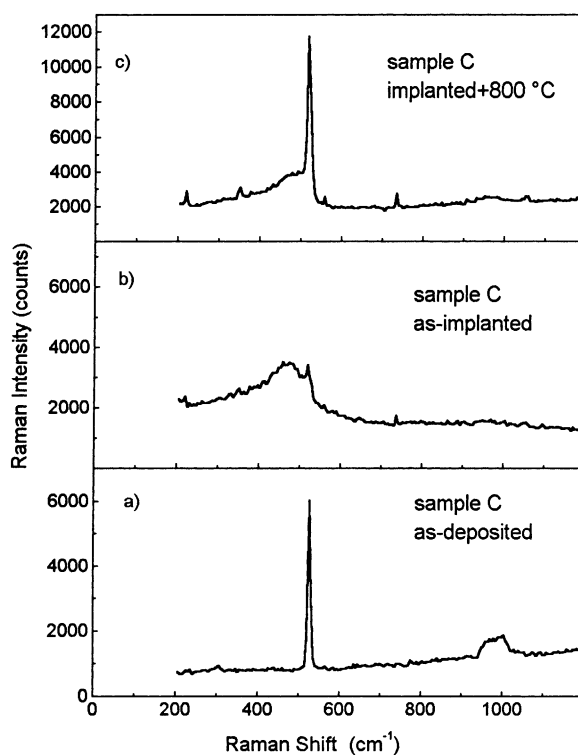


Fig. 5. Raman spectra for C series samples: (a) as-deposited; (b) as-implanted; (c) as-implanted and thermally treated at 800 °C.

downshift of SiO-bond stretching absorbance band, which is very sensitive to stoichiometry (ranging from about 1000 cm^{-1} in SiO to about 1080 cm^{-1} in SiO_2). Finally, the upshift of both peaks and the narrowing of this band after annealing at 800 °C suggest the occurrence of some structural rearrangement within the implanted layer yielding more tetrahedrally bonded Si–O.

The Raman spectrum of the as-deposited sample, shown in Fig. 5a, consists of two spectral components: the first one, peaked at about 520 cm^{-1} , is much more intense and narrow than the second one, which looks like a broad bump in the region between 920 and 1000 cm^{-1} . They are respectively due to the first- and second-order Raman scattering from the crystalline silicon of the substrate, since the as-deposited film is transparent to visible light: its refraction index ($n = 1.61$) is not too far from that of vitreous silica ($n_{\text{silica}} = 1.42$).

In the as-implanted samples (Fig. 5b), the broad and asymmetric bump, observed on the lower energy side

of the hardly observable c-Si peak at 520 cm^{-1} , is typical of non-crystalline Si phases. Despite of the important amorphisation caused to Si substrate by the heavy ion irradiation, the spectral features of this band (asymmetry, width and position of its maximum) are very similar to what can be observed in nano-crystalline silicon [13,14], thus suggesting the presence of Si nano-particles of various sizes. In fact, Si nano-clusters within the as-implanted films hinder the light penetration into the radiation damaged substrate, due to strong absorption of the blue light by silicon, so that even the first-order Raman scattering from c-Si wafer results hardly observable (Fig. 5b). Moreover, the presence of Si quantum dots in this sample immediately accounts for the observation of a room temperature intense photoluminescence band, centred around 670 nm (which cannot be related to amorphisation of Si substrate). Finally, this hypothesis is also consistent with the results of IR observations, which indicate substantial breaking of both SiH and SiO bonds and a concomitant presence of unbounded Si. The Raman spectrum after implantation and annealing at $800\text{ }^{\circ}\text{C}$ (Fig. 5c) consists of spectral components related to presence of both nano-crystalline Si and well-crystallised Si. In particular, the maximum of the spectral band related to nano-crystalline Si occurs at higher energy than in the as-implanted samples, suggesting the presence of bigger Si precipitates. Indeed, the treatment at $800\text{ }^{\circ}\text{C}$ after implantation is expected to cause an important agglomeration of Si nano-clusters, besides substantial structural recover of the radiation damaged substrate, which is reflected by the presence of both first- and second-order spectral components of c-Si in Fig. 5c.

Coming back to PAS, in the light of the above discussion and in accordance with the existing information regarding the behaviour of positron in irradiated SiO_2 [12], the decrease after implantation of the S parameter in the oxide can be ascribed to the reduction of Ps formation due to concomitant causes: (a) positron trapping at radiation-induced defects (e.g. damaged Si–O bonds and other charge-transfer centres); (b) reduction of the free volume associated to atomic rearrangement (Si cluster formation). The partial recovery of Ps formation after thermal treatments at 500 and $800\text{ }^{\circ}\text{C}$ comes from the annealing of the positron traps (broken bonds and charge-transfer centres in irradiated SiO_2 disappear at $600\text{ }^{\circ}\text{C}$ [9,15]).

Moreover, the residual H, which fills cavities that could host Ps, is progressively released during the thermal treatment.

The scenario becomes completely different after annealing at $1100\text{ }^{\circ}\text{C}$. At this temperature, the original SiO_x film evolves in a biphasic Si/SiO₂ mixture [4] formed by Si nano-crystals in a SiO₂ matrix. The S -value slightly below typical SiO₂ values probably indicates that positrons probe mainly the SiO₂ matrix and the interfacial defects with the Si nano-crystals, since a contribution from positron annihilation in the bulk of Si nano-crystals would bring S closer to one.

Further studies are planned to investigate: (i) the defects species detected by positrons; (ii) their role in the photoluminescence from the Si nano-structures; (iii) the role of the damage induced by ion bombardment in the formation of nano-structures.

Acknowledgements

This work was partially supported by the Ministero della Università e della Ricerca Tecnologica, Cofin 1998 program coordinated by Prof. G. Ottaviani. W.D. thanks INFM and R.F. the International Centre of Theoretical Physics for post-doctoral fellowships.

References

- [1] V. Vinciguerra, G. Franzò, F. Priolo, F. Iacona, C. Spinella, *J. Appl. Phys.* 87 (2000) 8165.
- [2] T. Shimizu-Iwayama, N. Kurumado, D.E. Hole, P.D. Townsend, *J. Appl. Phys.* 83 (1998) 6018.
- [3] T. Inokuma, Y. Wakayama, T. Muramoto, R. Aoki, Y. Kurata, S. Hasegawa, *J. Appl. Phys.* 83 (1998) 2228.
- [4] F. Iacona, G. Franzò, C. Spinella, *J. Appl. Phys.* 87 (2000) 1295.
- [5] M.V. Wolkin, J. Jorne, P.M. Fauchet, G. Allan, C. Delarue, *Phys. Rev. Lett.* 82 (1998) 197.
- [6] A. Sassella, A. Borghesi, F. Corni, A. Monelli, G. Ottaviani, R. Tonini, B. Pivac, M. Bacchetta, L. Zanotti, *J. Vac. Sci. Technol. A* 15 (1997) 377.
- [7] R.S. Brusa, G.P. Karwasz, M. Bettonte, A. Zecca, in: W.B. Waeber, M. Shi, A.A. Manuel (Eds.), *Slow Positron Beam Techniques for Solid and Surfaces*, Elsevier, Amsterdam, 1997, *Appl. Surf. Sci.* 116 (1997) 59.
- [8] A. Zecca, M. Bettonte, J. Paridaens, G.P. Karwasz, R.S. Brusa, *Meas. Sci. Technol.* 9 (1998) 1.
- [9] P. Asoka-Kumar, K.G. Lynn, D.O. Welch, *J. Appl. Phys.* 76 (1994) 4935.

- [10] A. Uedono, L. Wei, S. Tanigawa, R. Suzuki, H. Ohgaki, T. Mikado, T. Kawano, Y. Ohji, *J. Appl. Phys.* 75 (1994) 3822.
- [11] M. Clement, J.M.M. de Nijs, P. Balk, H. Schut, A. van Veen, *J. Appl. Phys.* 79 (1996) 9029.
- [12] M. Hasegawa, M. Saneyasu, M. Tabata, Z. Tang, Y. Nagai, T. Chiba, Y. Ito, *Nucl. Instrum. Meth. B* 166/167 (2000) 431.
- [13] S. Hayashi, T. Nagareda, Y. Kanzawa, K. Yamamoto, *Jpn. J. Appl. Phys.* 32 (1993) 3840–3845.
- [14] G. Mariotto, F.L. Freire Jr., F. Ziglio, *J. Non-Crystall. Sol.* 192/193 (1995) 253.
- [15] M. Fujinami, N.B. Chilton, *Appl. Phys. Lett.* 62 (1993) 1131.